International Journal of Engineering, Mathematical and Physical Sciences
ISSN: 2517-9934
Vol:6, No:1, 2012

Numerical Analysis of Hydrogen Transport using a Hydrogen-Enhanced Localized Plasticity Mechanism

Seul-Kee Kim, Chi-Seung Lee, Myung-Hyun Kim and Jae-Myung Lee

***Abstract*—**In this study, the hydrogen transport phenomenon was numerically evaluated by using hydrogen-enhanced localized plasticity (HELP) mechanisms. Two dominant governing equations, namely, the hydrogen transport model and the elasto-plastic model, were introduced. In addition, the implicitly formulated equations of the governing equations were implemented into ABAQUS UMAT user-defined subroutines. The simulation results were compared to published results to validate the proposed method.

***Keywords*—**Hydrogen-enhanced localized plasticity (HELP), Hydrogen embrittlement, Hydrogen transport analysis, ABAQUS UMAT, Finite element method (FEM).

I. Introduction

As the demand for hydrogen energy has continuously increased in recent decades, a design for safe high-pressure hydrogen transport/storage systems is required. The reservoirs and pipeline in hydrogen systems should be designed to endure high levels of internal pressure (more than 70 MPa). Under such circumstances, hydrogen-induced material degradation (e.g. hydrogen embrittlement, damage initiation/growth, etc.) commonly occurs [1]-[4], and these phenomena can cause catastrophic failure of hydrogen structures.

Recently, several mechanisms for the hydrogen embitterment have been proposed. Three types of mechanisms appear to be viable: stress-induced hydride formulation/cleavage [5], [6], hydrogen-induced decohesion [7], [8] and hydrogen-enhanced localized plasticity (HELP) [9]-[13].

According to the HELP theory, the presence of hydrogen in a solid solution increases the dislocation motion, which in turn increases the amount of plastic deformation that occurs in a localized region adjacent to the fracture zone [2].

One possible way through which the HELP mechanism can bring about macroscopic material failure is through hydrogen-induced cracking. Crack tip phenomena in hydrogen-induced cracking (e.g. hydrogen concentrations) are often based on the known details of the crack tip's elasto-plastic state.

[14] proposed a finite element (FE) model to demonstrate the effect of hydrostatic stress and trapping phenomena on the hydrogen distribution in plastically deformed steels. Based on their model, Krom et al. [15] proposed a formulation for achieving hydrogen balance by considering a strain rate factor in the hydrogen transport equation. [2], [16] and Miresmaeili et al. [17] used an FE scheme that differed from that of Krom et al. [15] and applied the Galerkin method in a 3D simulation to reconstruct the model of [14]. Taha and Sofronis [4] reviewed the progress by analyzing the material mechanical behaviour at a crack tip or round notch with that of hydrogen diffusion.

However, the developed code is based on in-house code and not on general-purpose FE programs. Considering the possible needs for numerical simulations of hydrogen-related failure in the near future, implementation of hydrogen transport equations in general-purpose FE programs is desirable.

Hence, the present paper describes the implementation of the hydrogen transport equation into the general-purpose FE program ABAQUS. The user-defined material subroutine UMAT was developed in order to calculate the important parameters related to hydrogen embrittlement (i.e. hydrostatic stress and plastic strain). Moreover, in order to validate the developed UMAT, the simulated results were compared with the results in the literature.

II. Hydrogen Diffusion Model

A. Hydrogen Transport Model

According to previous studies by Sofronis and McMeeking [14], hydrogen resides either at normal interstitial lattice sites (NILS) or at reversible trapping sites generated by plastic deformation [4]. The two populations are always in equilibrium according to Oriani's theory [7], [8]:

$$\frac{\theta_T}{1-\theta_T}=\frac{\theta_L}{1-\theta_L}\exp\left(\frac{W_B}{RT}\right) \tag{1}$$

Where θ_L and θ_T are the occupancies of the NILS and trapping sites, respectively, W_B is the trap binding energy, R is the gas constant equal to 8.31 J·mol^{-1}·K^{-1}, and T is the absolute temperature. The hydrogen concentration per unit volume in trapping sites C_T can be written as

$$C_T=\theta_T\alpha N_T \tag{2}$$

Seul-Kee Kim is with the Department of Naval Architecture and Ocean Engineering, Pusan National University, Busan 609-735 Republic of Korea, (phone: 82-51-510-3986; fax: 82-51-512-8836; e-mail: kfreek@pusan.ac.kr).

Chi-Seung Lee is with the Department of Naval Architecture and Ocean Engineering, Pusan National University, Busan 609-735 Republic of Korea, (phone: 82-51-510-3986; fax: +82-51-512-8836; e-mail: rich@pusan.ac.kr).

Myung-Hyun Kim is with the Department of Naval Architecture & Ocean Engineering, Pusan National University, Busan, South Korea, (phone: +82-51-510-2486; e-mail: kimm@pusan.ac.kr).

Jae-Myung Lee is with the Department of Naval Architecture and Ocean Engineering, Pusan National University, Busan 609-735 Republic of Korea, (phone: 82-51-510-2342; fax: 82-51-512-8836; e-mail: jaemlee@pusan.ac.kr).

Where α is the number of sites per trap and N_T, which is a function of the local effective plastic strain, is the trap density measured in number of traps per unit volume. The hydrogen concentration in NILS C_L can be expressed as

$$C_L = \theta_L \beta N_L \tag{3}$$

Where β is the number of NILS per solvent atom and N_L is the number of solvent lattice atoms per unit lattice volume. If the available number of trapping sites per unit volume, αN_T, is smaller than the available NILS per unit volume, βN_L, then

$$N_L = \frac{N_A}{V_M} \tag{4}$$

Where N_A (=6.0232×10^{23} atoms/mol) is Avogadro's number and V_M is the molar volume of the host lattice measured in units of volume per lattice mole.

Hydrogen conservation in any arbitrary material volume combined with Eqs. (2)– (4) yields the governing equation for transient hydrogen diffusion accounting for trapping and hydrostatic drift:

$$\frac{D_L}{D_{eff}}\frac{\partial C_L}{\partial t} = D_L \nabla^2 C_L + \nabla\left(\frac{D_L C_L V_H}{3RT}\nabla\sigma_{kk}\right) + \theta_T \frac{dN_T}{d\varepsilon_p}\frac{\partial \varepsilon_p}{\partial t} \tag{5}$$

Where D_L is the hydrogen diffusion constant through NILS and D_{eff} is an effective diffusion constant given by

$$D_{eff} = \frac{D_L}{\left(1+\frac{\partial C_T}{\partial C_L}\right)} \tag{6}$$

Here, V_H is the partial molar volume of hydrogen in solid solution and σ_{kk} is the hydrostatic stress which induces a drift for diffusion through the NILS.

B. Constitutive Model

In the presence of hydrogen, the hydrogen-induced lattice deformation should be modelled through the dilatational distortion that accompanies the introduction of the hydrogen solutes into the lattice. In order to incorporate the hydrogen-induced lattice deformation in the infinitesimal strain, the total strain rate should be calculated from

$$\dot{\varepsilon}_{ij} = \dot{\varepsilon}^e_{ij} + \dot{\varepsilon}^p_{ij} + \dot{\varepsilon}^t_{ij} \tag{7}$$

The terms in the above equation (from left to right) denote the total strain rate, elastic strain rate, plastic strain rate, and hydrogen-induced strain rate, respectively. The hydrogen-induced strain rate is purely dilatational and is given by

$$\dot{\varepsilon}^t_{ij} = \frac{1}{3}\frac{3V_H/V_M}{3+(c-c_0)V_H/V_M}\dot{c}\delta_{ij} \tag{8}$$

Where c is the total hydrogen concentration (in NILS and trapping sites) measured in hydrogen atoms per solvent atom, V_H is the hydrogen partial molar volume in solution and V_M is the molar volume of host metal.

As the hydrogen-induced strain rate is purely dilatational, it does not affect plastic strain and material hardening.

It is evident that the hydrogen diffusion is fully coupled with the stress analysis. For example, Eqs. (5) and (6) indicate that the calculation of the hydrogen distribution is coupled to the fields of the hydrostatic stress and effective strain. On the other hand, Eqs. (7) and (8) suggest that calculation of the plastic strains requires determining the hydrogen concentration.

The inelastic strain rate is calculated by using the Bodner-Partom elasto-(visco-) plastic model [18] as follows:

$$\dot{\varepsilon}^p_{ij} = D_0 \exp\left[-\frac{1}{2}\left(\frac{Z}{\sigma_{eff}}\right)^{2n}\right]\frac{\sqrt{3}S_{ij}}{\sigma_{eff}} \tag{9}$$

$$Z = Z_1 - (Z_1 - Z_0)\exp\left(-m\int \sigma_{ij} d\varepsilon^p_{ij}\right) \tag{10}$$

Where D_0 is the assumed maximum plastic strain rate, Z is the total hardening variable, and n is the material parameter that controls rate sensitivity. Z_0 and Z_1 are the initial and saturated values of the isotropic hardening variable, respectively; m is the rate of isotropic hardening.

III. Finite Element Implementation to ABAQUS

A. Numerical Algorithm of ABAQUS UMAT

In the present study, the aforementioned equations were transformed as an implicit form and implemented into the ABAQUS UMAT subroutine. In the UMAT subroutine, the hydrogen-induced strain rate is first calculated using Eqs. (7)–(11). The hydrogen concentration is then analyzed using Eqs. (1)–(6).

In the first step, the hydrostatic stress and effective plastic strain are calculated. In the next step, the hydrogen concentration is simultaneously calculated. From the calculated results, the stress-strain material nonlinear behaviour and hydrogen concentration distribution can be obtained.

The numerical algorithm of the UMAT subroutine is shown in Fig. 1.

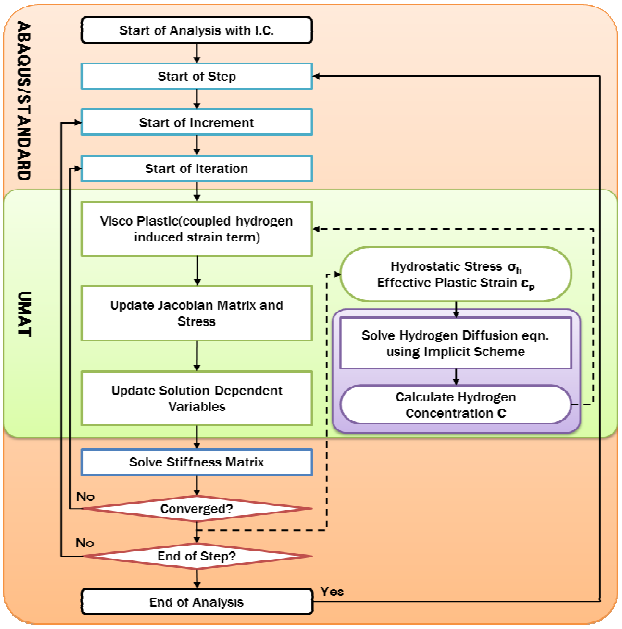

Fig. 1 Numerical algorithm of ABAQUS UMAT

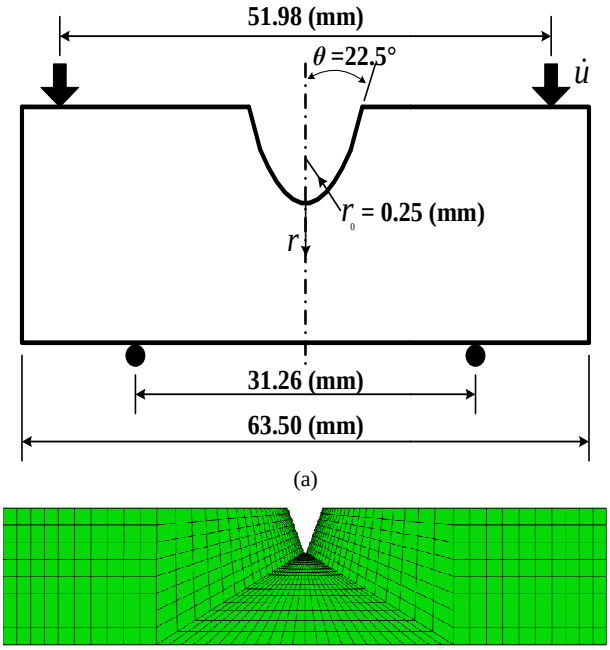

(a)

(b)

Fig. 2 (a) Description of the boundary and initial conditions for the coupled diffusion and elastic-plastic problem at a rounded-notch bend specimen under small scale yielding conditions [4] and (b) FE model

B. Finite Element Model

In order to validate the developed UMAT subroutine for hydrogen diffusion simulations, the analyzed results were compared with published results [4]. Fig. 2(a) shows the geometries of the test specimen. This is the rounded notch bend specimen. Fig. 2(b) shows the FE model of the test specimen. Four-node plane strain elements for the coupled temperature-displacement analysis (CPE4T in ABAQUS) were used. The numbers of elements and nodes were 1880 and 2418, respectively.

The yield strengths of low strength steel is 250 MPa. The elastic modulus is 207 GPa, and Poisson's ratio is 0.3.

C. Boundary and Loading Conditions

For the boundary conditions related to the hydrogen concentration, two types are introduced [1].

The first type is an 'environmental embrittlement' condition (BC Type I) which assumes that the specimen is under a uniform NILS hydrogen concentration $C_L = C_0$ at all times on the boundary of the specimen. The trapping site concentration C_T follows from the NILS population through Eqs. (1)–(4).

The second type is 'internal embrittlement' (BC Type II). At time $t = 0$, hydrogen is present in both the NILS and the trapping sites, and the two populations $C_L = C_0$ and C_T are in equilibrium according to Eqs. (1) – (4). For $t > 0$, all external surfaces, including those of the crack or notch, are assumed to be insulated. For all cases, the initial concentration C_0 was set to 2.084×10^{21} atom/m^3.

The loading conditions for the rounded notch bend specimen was performed by prescribing constant displacement rate until loading was complete ($t=t_l$). The prescribed displacement rate was 0.002mm/s. At times greater than t_l, the loading displacements were held constant and hydrogen diffusion continued under fixed held displacements.

IV. Numerical Examples and Discussions

The variations in the normalized concentration C_L/C_0 in NILS and C_T/C_0 in trapping sites with the normalized distance are shown in Fig. 3 for the rounded notch bend specimen with BC Type I (constant concentration condition) and BC Type II (zero hydrogen flux). The distance r (from the notch root) was normalized with respect to the initial notch radius r_0. In this figure, the results for $t = t_1$ indicate variation of C_L/C_0 and C_T/C_0 at time $t = t_1$, and the results for three different cases of t_1 (i.e. t_1 = 17 s, 40 s, 107 s) are shown. As shown in this figure, the FE analysis results agreed well with published results.

V. Concluding Remarks

In the present study, the hydrogen transport phenomenon was computationally analyzed on the basis of the HELP mechanism. Two dominant governing equations (i.e. the hydrogen transport model and the elasto-plastic model) were adopted. Moreover, the aforementioned models were transformed into the implicit form and implemented into an ABAQUS UMAT user-defined subroutine. The proposed UMAT was validated by comparison with published results for the hydrogen transport of the rounded notch bend specimen. The analysis results were confirmed to coincide well with published results.

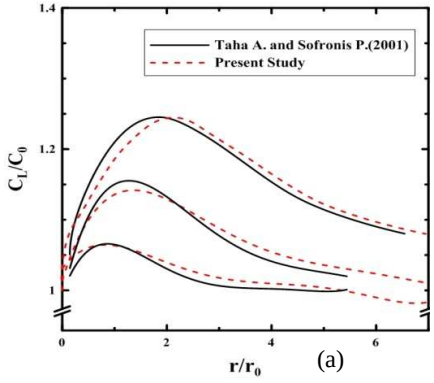

(a)

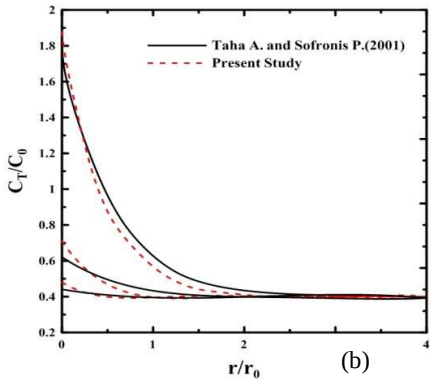

(b)

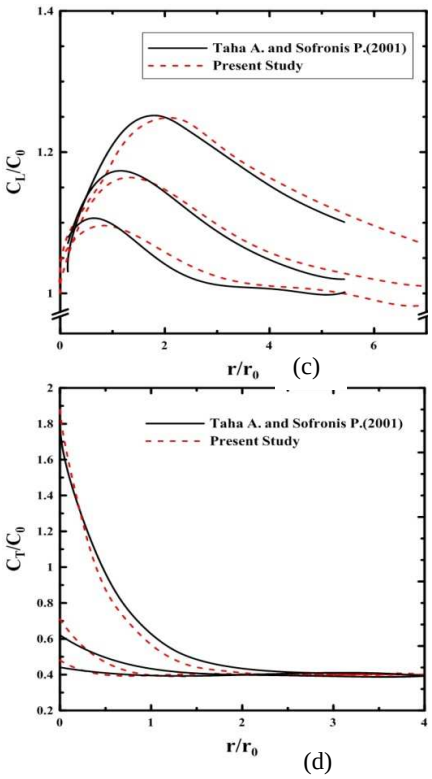

Fig. 3 Variations of the normalized concentration with the normalized distance for the boundary problem with BC Type I: (a) C_L/C_0 in NILS and (b) C_T/C_0 in trapping sites and with BC Type II: (c) C_L/C_0 in NILS and (d) C_T/C_0 in trapping sites

ACKNOWLEDGMENT

This research was supported by the Basic Science Research Program through the National Research Foundation of Korea (NRF) funded by the Ministry of Education, Science and Technology (2011-0004786).

REFERENCES

[1] C.S. Oh, Y.J. Kim, and K.B. Yoon, "Coupled analysis of hydrogen transport using ABAQUS," *J. Solid Mechanics and Materials Engineering*, vol. 4, 2010, pp. 908-917.
[2] H. Kanayama, M. Ogino, R. Miresmaeili, T. Nakagawa, and T. Toda, "Hydrogen transport in a coupled elastoplastic-diffusion analysis near a blunting crack tip," *J. Computational Science and Technology*, vol. 2, 2008, pp. 499-510.
[3] K. Takayama, R. Matsumoto, S. Taketomi, and N. Miyazaki, "Hydrogen diffusion analyses of a cracked steel pipe under internal pressure," *Int. J. Hydrogen Energy*, vol. 36, 2011, pp. 1037-1045.
[4] A. Taha and P. Sofronis, "A micromechanics approach to the study of hydrogen transport and embrittlement," *Engineering Fracture Mechanics*, vol. 68, 2001, pp. 803-837.
[5] J. Lufrano, P. Sofronis, and H.K. Birnbaum, "Modeling of hydrogen transport and elastically accommodated hydride formulation near a crack tip," *J. Mechanics and Physics of Solids*, vol. 44, 1996, pp. 179-205.
[6] J. Lufrano, P. Sofronis, and H.K. Birnbaum, "Elastoplastically accommodated hydride formulation and embrittlement," *J. Mechanics and Physics of Solids*, vol. 46, 1998, pp. 1497-1520.
[7] R.A. Oriani, and P.H. Josephic, "Equilibrium aspects of hydrogen-induced cracking of steels," *Acta Metallurgica*, vol. 22, 1974, pp. 1065-1074.
[8] R.A. Oriani, and P.H. Josephic, "Equilibrium and kinetic studies of the hydrogen-assisted cracking of steel," *Acta Metallurgica*, vol. 25, 1977, pp. 979-988.
[9] S.M. Myers, M.I. Baskes, H.K. Birnbaum, J.W. Corbett, G.G. Deleo, S.K. Estreicher, E.E. Haller, P. Jena, N.M. Johnson, and R. Kirchheim, "Hydrogen interaction with defects in crystalline solids," *Reviews of Modern Physics*, vol. 64, 1992, pp. 559-617.
[10] T. Tabata, and H.K. Birnbaum, "Direct observation of the effect of hydrogen on the behavior of dislocations in iron," *Scripta Metallurgica*, vol. 17, 1983, pp. 947-950.
[11] H.K. Birnbaum, and P. Sofronis, "Hydrogen-enhanced localized plasticity - a mechanism for hydrogen-related fracture," *Materials Science and Engineering A*, vol. 176, 1994, pp. 191-202.
[12] H.K. Birnbaum, "Hydrogen effects on deformation – Relation between dislocation behavior and the macroscopic stress-strain behavior," *Scripta Metallurgica et Materialia*, vol. 31, 1994, pp. 149-153.
[13] P. Sofronis, and H.K. Birnbaum, "Mechanics of the hydrogen-dislocation-impurity interactions – I. Increasing shear modulus," *J. Mechanics and Physics of Solids*, vol. 43, 1995, pp. 49-90.
[14] P. Sofronis, R.M. McMeeking, "Numerical analysis of hydrogen transport near a blunting crack tip," *J. Mechanics and Physics of Solids*, vol. 37, 1989, pp. 317-350.
[15] A.H.M. Krom, R.W.J. Koers, and A. Bakker, "Hydrogen transport near a blunting crack tip," *J. Mechanics and Physics of Solids*, vol. 47, 1999, pp. 971-992.
[16] H. Kanayama, T. Shingoh, S. Ndong-Mefane, M. Ogino, R. Shioya, and H. Kawai, "Numerical analysis of hydrogen diffusion problems using the finite element method," *Theoretical and Applied Mechanics Japan*, vol. 56, 2008, pp. 389-400.
[17] R. Miresmaeili, M. Ogino, T. Nakagawa, and H. Kanayama, "A coupled elastoplastic-transient hydrogen diffusion analysis to simulate the onset of necking in tension by using the finite element method," *Int. J. Hydrogen Energy*, vol. 35, 2010, pp. 1506-1514.
[18] S.R. Bodner *Unified Plasticity for Engineering Applications*, New York, Kluwer Academic and Plenum Publishers, 2002, pp. 1-114.